# Carbon-11-Labeled KF15372: A Potential Central Nervous System Adenosine $A_1$ Receptor Ligand

Riko Furuta, Kiichi Ishiwata, Motohiro Kiyosawa, Shin-ichi Ishii, Noriko Saito, Jun-ichi Shimada, Kazutoyo Endo, Fumio Suzuki and Michio Senda

*Positron Medical Center, Tokyo Metropolitan Institute of Gerontology; Showa College of Pharmaceutical Sciences; Department of Ophthalmology, Tokyo Medical and Dental University; Tokyo, Japan; and Pharmaceutical Research Laboratories, Kyowa Hakko Kogyo Co., Shizuoka, Japan*

The carbon-11-labeled selective adenosine $A_1$ antagonist KF15372 ([1-propyl-$^{11}$C]8-dicyclopropylmethyl-1,3-dipropylxanthine) was evaluated in vivo as a PET ligand for mapping CNS adenosine $A_1$ receptors. **Methods:** The regional brain distribution of [$^{11}$C]KF15372 and the effects of adenosine antagonists on the distribution were determined in mice by tissue sampling. In rats, in which the retinal projection fibres to the superior colliculus had degenerated due to unilateral eye removal, the brain distribution of [$^{11}$C]KF15372 was visualized by ex vivo autoradiography. **Results:** The mouse brain uptake of [$^{11}$C]KF15372 was 1.8% i.d./g at 5 min and then it gradually decreased. The uptake was high in the hippocampus, cerebral cortex, striatum and cerebellum, and was significantly reduced by $A_1$ antagonists but not by $A_2$ antagonists. The brain distribution of $^{11}$C assessed by the tissue sampling and autoradiography was compatible with that of the $A_1$ receptors. Autoradiography clearly visualized unilaterally decreased $A_1$ receptor binding in the superior colliculus. **Conclusion:** The results demonstrated that [$^{11}$C]KF15372 is a selective and high-affinity adenosine $A_1$ receptor ligand and is useful for detecting the degeneration of presynaptic neurons.

**Key Words:** adenosine; PET; carbon-11-KF15372; $A_1$ receptor; presynaptic neuron

**J Nucl Med 1996; 37:1203–1207**

Adenosine is present in large amounts in the mammalian brain. Adenosine is an endogenous modulator that mediates the effect of general depression of central nervous system (CNS) activity (*1–3*). The biological effects of adenosine are mediated via interaction with at least two classes of adenosine receptors designated $A_1$ and $A_2$. $A_1$ receptors have relatively high affinity for adenosine and act on adenylate cyclase in an inhibitory manner, while $A_2$ receptors have lower affinity for adenosine and stimulate adenylate cyclase. It is now known that $A_1$ receptors are G protein-linked and can act through effectors other than adenylate cyclase, including potassium channels, calcium channels, phospholipases $A_2$ and C and guanylate cyclase (*2*).

$A_1$ receptors are present throughout the presynaptic region of excitatory neurons (*4–10*), being rich in the hippocampus, cerebral cortex, thalamic nuclei, the basal ganglia and the cerebellar cortex in animals (*11–14*) and humans (*15*). Extracellular adenosine may control the synaptic transmission in the CA1 region of the hippocampus (*16*).

PET has been applied to studies of ligand receptor interactions and has provided a significant amount of information about the neurochemistry of neurodegenerative disorders (*17,18*). Considering the physiological roles of adenosine and its receptors, the visualization of $A_1$ receptors by PET could provide a new tool for evaluation of presynaptic function of the CNS and damage in brain disorders.

Some xanthine derivatives are selective and high-affinity $A_1$ antagonists and have been proposed as therapeutic agents for cognitive deficits and renal failure (*2,3*). We (*19*) synthesized $^{11}$C-labeled 8-dicyclopropylmethyl-1,3-dipropylxanthine (KF15372, Fig. 1), a potent $A_1$ antagonist (a Ki value for the $A_1$ receptor is 3.0 n*M*) (*20*). The mouse brain uptake of the [$^{11}$C]KF15372 was significantly higher than that of the weaker antogonist 7-[$^{11}$C]methyl-KF15372, and reduced by the co-injected carrier KF15372 but not by an $A_2$ antagonist (*19*). The aim of this study was to evaluate the potential of [$^{11}$C]KF15372 as a PET radioligand for mapping CNS adenosine $A_1$ receptors. We investigated the regional brain distribution of the [$^{11}$C]KF15372 in mice and the effect of adenosine antagonists on the distribution. Ex vivo autoradiography revealed the degeneration of presynaptic neurons in the rat model with unilateral eye removal.

## MATERIALS AND METHODS

8-Dicyclopropylmethyl-1,3-dipropylxanthine (KF15372) and (*E*)-1,3-dipropyl-8-(3,4-dimethoxystyryl)-7-methylxanthine (KF17837) were prepared as described (*20–22*). 8-Cyclopentyl-1,3-dipropylxanthine (DPCPX) and 3,7-dimethyl-1-propargylxanthine (DMPX) were used in this study. Caffeine was also used.

### Radiosynthesis

Carbon-11 KF15372 was synthesized as described (*19*) (Fig. 1). Briefly, [$^{11}$C]propyl iodide was trapped in 0.2 ml of dry DMF containing 1 mg of the 1-despropyl compound and 2 mg of NaH. The solution was heated at 110°C for 5 min. After adding 1.0 ml of 0.1 M HCl, the solution was loaded onto an ODS column (20 mm i.d. × 150 mm), and eluted with a mixture of acetonitrile and water (45/55, v/v) at a flow rate of 20 ml/min. The [$^{11}$C]KF15372 fraction (retention time: 13~14 min) was evaporated to dryness. The residue was dissolved in physiological saline containing Tween 80, and its membrane filtration produced radiochemically pure [$^{11}$C]KF15372 with a specific radioactivity of 10~56 GBq/μmole.

### Biodistribution Study

Male ddY mice (33~39 g) were divided into four groups. The first group was intravenously injected with [$^{11}$C]KF15372 (300~650 kBq/50~100 pmole) and killed by cervical dislocation 5, 15, 30 and 60 min postinjection. The blood was collected by heart puncture and the tissues were harvested. Samples were then assayed for $^{11}$C in an auto-gamma counter and weighed. The tissue uptake of $^{11}$C was expressed as the percent injected dose per gram of tissue.

The second group was also injected intravenously but with [$^{11}$C]KF15372 together with one of the following four adenosine antagonists (1-to-100 nmole/animal): selective adenosine $A_1$ antagonists KF15372 and DPCPX and selective $A_2$ antagonists

Received Mar. 29, 1995; revision accepted Nov. 8, 1995.

For correspondence or reprints contact: Kiichi Ishiwata, PhD, Positron Medical Center, Tokyo Metropolitan Institute of Gerontology, 1-1 Naka-cho, Itabashi, Tokyo 173, Japan.

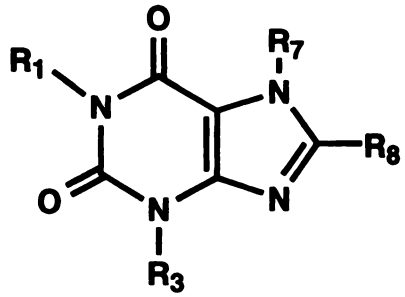

[$^{11}$C]KF15372: $R_1$, $CH_3CH_2{}^{11}CH_2$; $R_3$, *n*-Pr; $R_7$, H; $R_8$, dicyclopropylmethyl

DPCPX: $R_1$, *n*-Pr; $R_3$, *n*-Pr; $R_7$, H; $R_8$, cyclopentyl

KF17837: $R_1$, *n*-Pr; $R_3$, *n*-Pr; $R_7$, Me; $R_8$, 3,4-dimethoxystyryl

DMPX: $R_1$, propargyl; $R_3$, Me; $R_7$, Me; $R_8$, H

caffeine: $R_1$, Me; $R_3$, Me; $R_7$, Me; $R_8$, H

**FIGURE 1.** Chemical structures of [$^{11}$C]KF15372 and adenosine antagonists.

DMPX and KF17837. The brain uptake was measured 15 min after injection.

The third group was administered [$^{11}$C]KF15372 intravenously together with carrier KF15372 (100 nmole/animal), and the regional brain distribution was determined at 5, 15 and 30 min later by standard procedures. The brain was divided into the cerebral cortex, hypothalamus, hippocampus, striatum, midbrain, medulla oblongata and cerebellum (*23*).

In the fourth group of mice, the effects of co-injected adenosine antagonists (100 nmole/head): DPCPX, DMPX, KF17837 or the nonselective antagonist caffeine on the regional brain distribution were measured after 15 min.

### Metabolite Study

Mice were intravenously injected with [$^{11}$C]KF15372 (10~14 MBq/0.3~0.6 nmole), and killed by cervical dislocation at 5, 15 and 30 min postinjection. Long-Evans rats (56~76 g) were injected intravenously with [$^{11}$C]KF15372 (75~90 MBq/2.7~3.7 nmole), and killed 15 min later. The cerebral cortex or cerebellum was homogenized in 1 ml of 10% trichloroacetic acid in acetonitrile/water (4/6, v/v). After centrifugation at 7000 g for 2 min, the precipitate was resuspended in the same solvent followed by centrifugation. This procedure was repeated once. The plasma was denatured with an equivalent volume of 20% trichloroacetic acid in acetonitrile. The mixture was processed as described above. Over 98% of the radioactivity was recovered in the supernatant. Combined supernatants of the cortex, cerebellum or plasma were loaded onto a Nova-pak C18 column equipped in an RCM 8 × 10 module (8 mm × 100 mm, Waters) and eluted with a mixture of acetonitrile and 3% triethylamine-$H_3PO_4$ (pH 2.0) (4/6, v/v) at a flow rate of 2 ml/min. The elution profile was detected with a radioactivity monitor, and the amount of radioactivity in 1 or 2 ml was measured with an auto-gamma counter. Recovery of the radioactivity was essentially quantitative.

### Autoradiography Study

At postnatal Day 10, Long-Evans rats (17~23 g) were anesthetized and the right eye was removed. At 10, 14 and 20 days later, the rats were killed 15 min after intravenous injection of [$^{11}$C]KF15372 (75~90 MBq/2.5~3.7 nmole). The brain was rapidly dissected, frozen and cut coronally into 20-$\mu$m thick sections using a cryotome at −15°C. The sections were mounted on glass slides, dried on a hot plate at 60°C and apposed to an imaging plate.

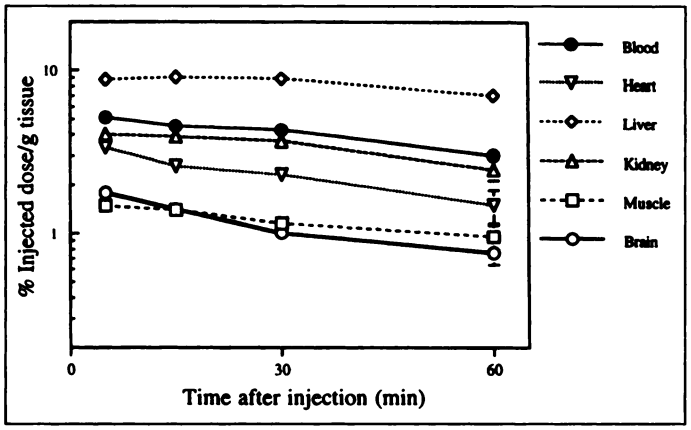


**FIGURE 2.** Tissue distribution of radioactivity in mice after an intravenous injection of [$^{11}$C]KF15372 with and without carrier KF15372. Mean ± s.d. (n = 4).

## RESULTS

### Biodistribution Study

A high uptake of [$^{11}$C]KF15372 was found in the liver followed by the kidney, heart, muscle and brain (Fig. 2). The $^{11}$C levels of all these tissues gradually decreased. The blood clearance rate was slow and the brain-to-blood ratio was 0.25~0.34.

Figure 3 shows the effects of co-injected doses of adenosine antagonists on the whole brain uptake of [$^{11}$C]KF15372. The uptake decreased depending on the dose of carrier KF15372 and $A_1$ antagonist DPCPX, whereas $A_2$ antagonists DMPX and KF17837 scarcely affected the brain uptake.

In the brain, the uptake of [$^{11}$C]KF15372 was high in the hippocampus, cerebral cortex, striatum and cerebellum (Table 1). The $^{11}$C levels gradually decreased in all regions. The co-injection of carrier KF15372 significantly reduced the uptake at all three time points and in all brain regions sampled, in which the $^{11}$C levels were comparable.

As shown in Figure 4, the uptake of [$^{11}$C]KF15372 was significantly reduced in all brain regions by co-injection of the $A_1$ antagonist DPCPX. On the other hand, little effect was found when $A_2$ antagonist DMPX or KF17837, or the nonselective weak antagonist caffeine was injected.

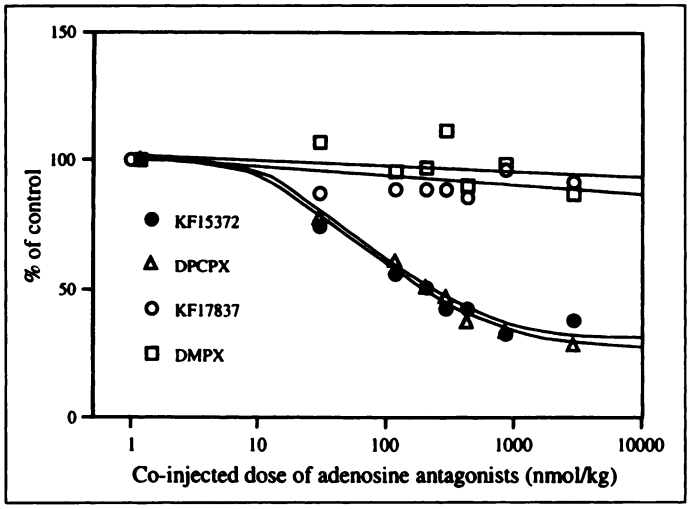


**FIGURE 3.** Effect of a loading dose of adenosine antagonists on the brain uptake 15 min after intravenous injection [$^{11}$C]KF15372 into mice. The brain uptake was normalized as a percentage of the respective control (mean, n = 4).

**TABLE 1**
Regional Brain Distribution of Carbon-11-KF15372 in Mice and the Effect of Carrier KF15372 on the Distribution

| | %ID/g tissue control<br>carrier KF15372 | | |
|---|---|---|---|
| | 5 min | 15 min | 30 min |
| Cerebral cortex | 2.00 ± 0.14<br>1.03 ± 0.06‡ | 1.83 ± 0.28<br>1.23 ± 0.16‡ | 0.83 ± 0.19<br>0.34 ± 0.07† |
| Hypothalamus | 1.40 ± 0.16<br>0.97 ± 0.11† | 1.49 ± 0.18<br>0.88 ± 0.30† | 0.91 ± 0.26<br>0.40 ± 0.25† |
| Striatum | 2.09 ± 0.22<br>1.14 ± 0.23‡ | 2.08 ± 0.30<br>0.89 ± 0.27† | 1.25 ± 0.52<br>0.35 ± 0.12* |
| Hippocampus | 1.84 ± 0.20<br>1.21 ± 0.21† | 1.81 ± 0.28<br>1.26 ± 0.16‡ | 1.39 ± 0.48<br>0.69 ± 0.23* |
| Midbrain | 1.77 ± 0.10<br>0.96 ± 0.07‡ | 1.34 ± 0.33<br>0.51 ± 0.09‡ | 0.75 ± 0.15<br>0.34 ± 0.09† |
| Medulla oblongata | 1.56 ± 0.26<br>1.02 ± 0.08† | 1.31 ± 0.15<br>0.73 ± 0.13‡ | 0.65 ± 0.12<br>0.40 ± 0.13* |
| Cerebellum | 2.00 ± 0.18<br>1.09 ± 0.04‡ | 1.64 ± 0.40<br>0.95 ± 0.15‡ | 0.85 ± 0.07<br>0.38 ± 0.07‡ |

Injected carrier KF15372: 100 nmole/animal. Mean ± s.d. (n = 4~5). Student's t-test was performed to evaluate the control and the group given carrier: *$p < 0.05$, †$p < 0.01$ and ‡$p < 0.001$.

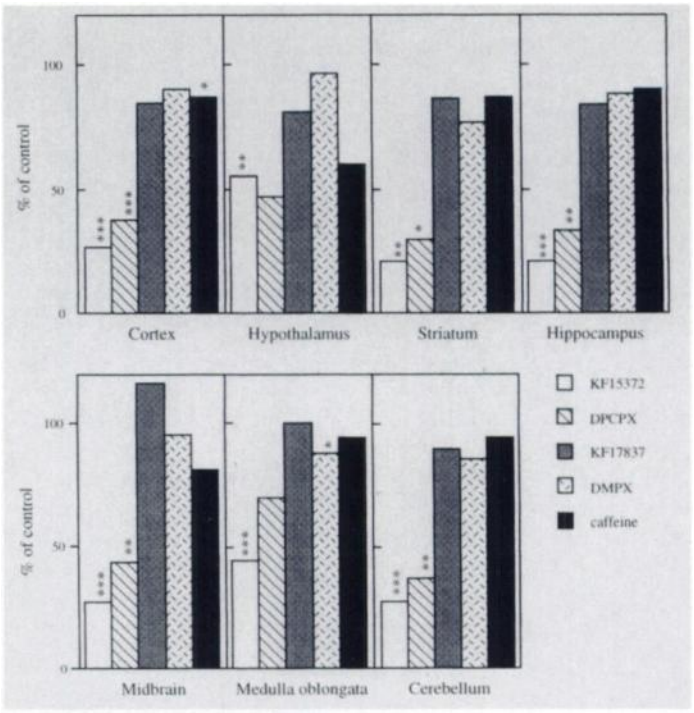


**FIGURE 4.** Effects of adenosine antagonists on the regional brain distribution of [$^{11}$C]KF15372 at 15 min after an intravenous injection into mice. The injected dose of each antagonist was 100 nmole/animal. The brain uptake was normalized as percentage of the respective control (mean, n = 4). Student's t-test was performed between the control and each group: *$p < 0.05$, **$p < 0.01$ and ***$p < 0.001$.

### Metabolite Study

In the HPLC analysis of plasma, besides [$^{11}$C]KF15372 (retention time of 10 min), unidentified labeled metabolites one and two were detected at retention times of 4.1 and 7.0 min, respectively. As shown in Table 2, the labeled metabolites increased with time in the plasma. In the cerebral cortex and cerebellum, metabolites one and two were also detected. At 15 min after the injection 90% of the $^{11}$C was detected as [$^{11}$C]KF15372 in both mice and rats.

### Autoradiography Study

Figures 5 and 6 show the autoradiography images of the brain sections of the rats that had undergone the right unilateral orbital enucleation. The highest $^{11}$C density was found in the cerebral cortex, thalamus (LD, MD and V), hippocampus (CA1 and CA3), lateral geniculate complex (LG), medial geniculate nucleus (MG) and cerebellar cortex (molecular layer, Mol). As clearly shown in Figure 6, a high density of $^{11}$C was also observed in the superior colliculus of the right hemisphere (the left side in the images), whereas the density in the left hemisphere of the superior colliculus was greatly diminished at 7, 14 and 20 days postenucleation.

## DISCUSSION

The evidence presented here suggested that [$^{11}$C]KF15372 is a selective and high-affinity adenosine $A_1$ ligand in vivo and useful for detecting the degeneration of presynaptic neurons.

Tissue sampling showed that the regional brain distribution of [$^{11}$C]KF15372 was consistent with that of $A_1$ receptors (*11–14*). The ex vivo autoradiograms (Fig. 5) were similar to the in vitro autoradiogram obtained with [$^3$H]cyclohexyladenosine (*14*). The levels of [$^{11}$C]KF15372 gradually decreased in all brain regions, suggesting reversibility of the tracer or relatively low affinity in vivo. We point out that the $A_1$ receptor selective uptake was even observed at 5 min after injection. The selectivity of [$^{11}$C]KF15372 for the $A_1$ receptors was demonstrated by the fact that the brain uptake was reduced by the $A_1$ antagonists KF15372 and DPCPX, but not by the $A_2$ antagonists KF17837 and DMPX. Because of weak affinity (Ki, >100 $\mu M$) (*20*), the nonselective antagonist caffeine did not result in a significant reduction in the brain uptake. The results indicated

**TABLE 2**
Percentages of Labeled Metabolites of Carbon-11-KF15372 in Mice and Rats

| | | Metabolites (%) | | |
|---|---|---|---|---|
| | | Metabolite 1 | Metabolite 2 | [$^{11}$C]KF15372 |
| Plasma | Mouse | | | |
| | 5 min | 38.0 ± 2.0 | 1.7 ± 2.0 | 60.2 ± 4.0 |
| | 15 min | 53.5 ± 6.7 | 3.0 ± 1.0 | 37.7 ± 2.7 |
| | 30 min | 64.9 ± 12 | 1.7 ± 0.9 | 14.4 ± 4.6 |
| Plasma | Rat | | | |
| | 15 min | 53.7 ± 2.1 | 1.2 ± 0.4 | 32.8 ± 6.8 |
| Cerebral cortex | Mouse | | | |
| | 5 min | 7.0 ± 2.5 | 0.1 ± 0.1 | 92.9 ± 2.4 |
| | 15 min | 7.0 ± 2.5 | 0.8 ± 0.8 | 91.3 ± 2.1 |
| | 30 min | 21.1 ± 6.9 | 0.4 ± 0.6 | 80.9 ± 2.5 |
| | Rat | | | |
| | 15 min | 8.1 ± 2.6 | 0.8 ± 1.0 | 89.6 ± 2.8 |
| Cerebellum | Mouse | | | |
| | 5 min | 4.9 ± 0.6 | nd | 95.1 ± 0.6 |
| | 15 min | 8.5 ± 3.2 | 0.8 ± 0.7 | 90.2 ± 3.8 |
| | 30 min | 20.3 ± 4.7 | 1.5 ± 2.6 | 78.3 ± 2.3 |
| | Rat | | | |
| | 15 min | 6.9 ± 2.0 | 0.4 ± 0.5 | 91.9 ± 3.1 |

Mean ± s.d. (n = 3). nd; not detected.

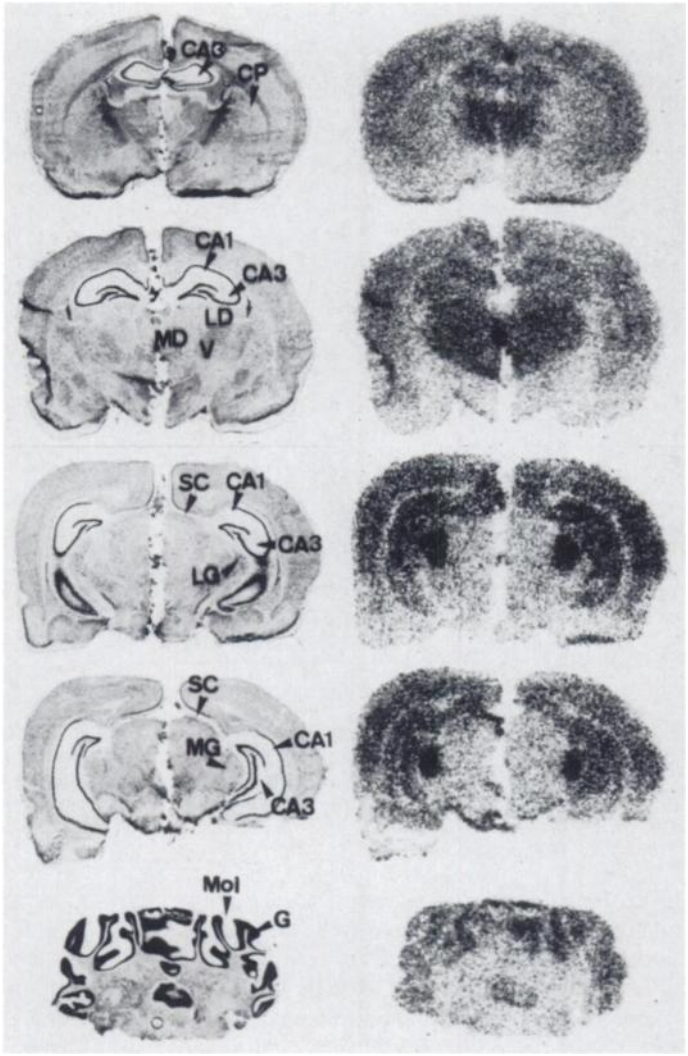


**FIGURE 5.** Autoradiograms of the brain sections at 15 min after intravenous injection of [$^{11}$C]KF15372 into a rat at 20 days after unilateral eye removal. Left images show cresyl violet staining, and the right represents autoradiographic images. The right hand hemisphere of the brain was located in the left of each image. CA1 and CA3, CA1 and CA3 subfields of the hippocampus; CP = caudate putamen; G = granule cell layer of cerebellar cortex; LD = laterodorsal thalamic nucleus; LG = lateral geniculate complex; MD = mediodorsal thalamic nucleus; MG = medial geniculate nucleus; Mol = molecular layer of cerebellar cortex; SC = superior colliculus; V = ventral thalamic nuclei.

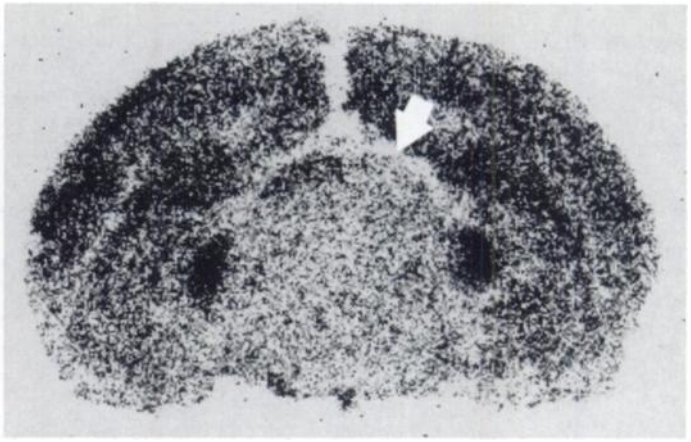

**FIGURE 6.** Autoradiograms of rat brain sections 15 min after an intravenous injection of [$^{11}$C]KF15372 14 days after unilateral eye removal. Arrow indicates the marked decreased uptake of [$^{11}$C]KF15372 in the left superior colliculus connected to the right enucleated eye.

that [$^{11}$C]KF15372, a ligand which displays 140-fold higher affinity for $A_1$ than $A_2$ receptors in vitro (*20*), can also distinguish between these receptors in vivo.

In the metabolite study, the presence of labeled metabolites of [$^{11}$C]KF15372 in the brain tissues can be explained in two ways. The [$^{11}$C]KF15372 was degraded peripherally to metabolites, which were transferred from plasma to brain tissue. Otherwise, the metabolites were produced in the brain tissue. Considering the metabolism of caffeine and the retention times of labeled metabolites in the HPLC, the metabolites may be hydrophilic compounds such as desalkylated KF15372 and hydroxylated compounds.

Another potential disadvantage of this compound in vivo is the low brain-to-blood ratios of the radioactivity. As indicated (*19*), [$^{11}$C]KF15372 was present in the plasma but not taken up by blood cells. Lipophilicity of the compound facilitated the penetration of the blood-brain barrier, whereas the binding to the plasma proteins probably interferes with absorption of the compound by the organs. In spite of these disadvantageous properties, the usefulness of [$^{11}$C]KF15372 was demonstrated by the ex vivo autoradiography, in which we used a rat model in which the right eye was enucleated (*5,25,26*). The rat has a well-developed retinotectothalamocortical system in the visual system. The majority of retinal impulses (65%) are transmitted to the superior colliculus (*27*). $A_1$ receptors are abundant in the synaptic terminals of retinal projection fibers (*5,25*). Retinal projection fiber loss reaches a maximum at seven days after eye removal (*26*). Therefore, the reduced uptake of [$^{11}$C]KF15372 in the left superior colliculus which receives visual input from the enucleated right eye (Figs. 5, 6), indicates a loss of $A_1$ receptors in the presynaptic terminal. The images reflect degeneration of the retinal projection fibers.

Because of localization of the $A_1$ receptors in the presynaptic membranes, PET studies with [$^{11}$C]KF15372 possibly assess the activities in the presynaptic neurons, as demonstrated above by the ex vivo autoradiography study. On the other hand, the activities in the postsynaptic neurons are usually assessed by other tracers measuring glucose metabolism ([$^{18}$F]fluorodeoxyglucose) and blood flow ([$^{15}$O]water or [$^{15}$O]$CO_2$). Therefore, trans-synaptic processes neuroanatomically associated with neuronal damage or degeneration could be evaluated by PET. Recently, Nagasawa et al. reported that alteration of the $A_1$ receptors binding was involved in ischaemic foci as well as in remote areas outside them (*28*).

## CONCLUSION

Tissue sampling and ex vivo autoradiography suggest that the regional brain distribution of [$^{11}$C]KF15372 is consistent with that of the adenosine $A_1$ receptors found in mice and rats. The brain uptake of the [$^{11}$C]KF15372 was competitively reduced by the co-administration of $A_1$, but not $A_2$ antagonists. The ex vivo autoradiography on the rat model with unilateral orbital enucleation, visualized the $A_1$ receptor deficiency in the presynaptic terminals. These pieces of evidence demonstrated the potential of [$^{11}$C]KF15372 as a radioligand mapping for CNS adenosine $A_1$ receptors.

## ACKNOWLEDGMENTS

The authors thank Dr. S. Shibabe for advice and discussions regarding the autoradiography studies, the Radioisotope School Nuclear Education Center, Japan Atomic Energy Research Institute (Tokyo, Japan), where the autoradiography was analyzed. The authors also thank Dr. K. Ishii (TMIG) for useful discussion.

## REFERENCES

1. Olsson RA, Pearson JD. Cardiovascular purinoceptors. *Physiol Rev* 1990;70:761–854.
2. Collis MG, Hourani SMO. Adenosine receptor subtypes. *Trends Pharmacol Sci* 1993;14:360–366.
3. Suzuki F. Adenosine $A_1$ antagonists; a new therapeutic approach to cognitive deficits and acute renal failure. *Drug News Perspect* 1992;5:587–591.
4. Goodman RR, Kuhar MJ, Hester L, Snyder SH. Adenosine receptors: autoradiographic evidence for their location on axon terminals of excitatory neurons. *Science* 1983;220: 967–969.
5. Silinski EM. On the mechanism by which adenosine receptor activation inhibits the release of acetylcholine from motor nerve ending. *J Physiol* 1984;346:243–256.
6. Dunwiddie TV, Haas HL. Adenosine increases synaptic facilitation in the in vitro rat hippocampus: evidence for a presynaptic site of action. *J Physiol* 1985;369:365–377.
7. Lupica CR, Proctor WR, Dunwiddie TV. Presynaptic inhibition of excitatory synaptic transmission by adenosine in rat hippocampus: analysis of unitary EPSP variance measured by whole-cell recording. *J Neurosci* 1992;12:3753–3764.
8. Prince DA, Stevens CF. Adenosine decreases neurotransmitter release at central synapses. *Proc Natl Acad Sci USA* 1992;89:8586–8590.
9. Scanziani M, Capogna M, Gahwiler BH, Thompson SM. Presynaptic inhibition of miniature excitatory synaptic currents by baclofen and adenosine in the hippocampus. *Neuron* 1992;9:919–927.
10. Scholz KP, Miller RJ. Inhibition of quantal transmitter release in the absence of calcium influx by a G protein-linked adenosine receptor at hippocampal synapses. *Neuron* 1992;8:1139–1150.
11. Lewis ME, Patel J, Moon Edley S, Marangos PJ. Autoradiographic visualization of rat brain adenosine receptors using N6-cyclohexyl[$^3$H]adenosine. *Eur J Pharmacol* 1981;73:109–110.
12. Goodman RR, Snyder SH. Autoradiographic localization of adenosine receptors in rat brain using [$^3$H]cyclohexyladenosine. *J Neurosci* 1982;2:1230–1241.
13. Pagonopoulou O, Angelatou F, Kostopoulos G. Effect of pentylentetrazol-induced seizures on $A_1$ adenosine receptor regional density in the mouse brain: a quantitative autoradiographic study. *Neuroscience* 1993;56:711–716.
14. Fastbom J, Pazos A, Palacios JM. The distribution of adenosine $A_1$ receptors and 5′-nucleotidase in the brain of some commonly used experimental animals. *Neuroscience* 1987;22:813–826.
15. Fastbom J, Pazos A, Probst A, Palacios JM. Adenosine $A_1$ receptors in the human brain: a quantitative autoradiographic study. *Neuroscience* 1987;22:827–839.
16. Manzoni OJ, Manabe T, Nicoll RA. Release of adenosine by activation of NMDA receptors in the hippocampus. *Science* 1994;265:2098–2101.
17. Frost JJ. Imaging neuronal biochemistry by emission computed tomography: focus on neuroreceptors. *Trends Pharmacol Sci* 1986;7:490.
18. Mazière B, Mazière M. Where have we got to with neuroreceptor mapping of the human brain? *Eur J Nucl Med* 1990;16:817–835.
19. Ishiwata K, Furuta R, Shimada J, et al. Synthesis and preliminary evaluation of [$^{11}$C]KF15372, a selective adenosine $A_1$ antagonist. *Appl Radiat Isot* 1995;46:1009–1013.
20. Shimada J, Suzuki F, Nonaka H, et al. 8-(Dicyclopropylmethyl)-1,3-dipropylxanthine: a potent and selective adenosine $A_1$ antagonist with renal protective and diuretic activities. *J Med Chem* 1991;34:466–469.
21. Suzuki F, Shimada J, Mizumoto H, et al. Adenosine $A_1$ antagonists. II. Structure-activity relationships on diuretic activities and protective effects against acute renal failure. *J Med Chem* 1992;35:3066–3075.
22. Shimada J, Suzuki F, Nonaka H, Ishii A, Ichikawa S. (*E*)-1,3-Dialkyl-7-methyl-8-(3,4,5-trimethoxystyryl)xanthines: potent and selective adenosine $A_2$ antagonists. *J Med Chem* 1992;35:2342–2345.
23. Glowinski J, Iversen LL. Regional studies of catecholamines in the brain. I. The disposition of [$^3$H]norepinephrine, [$^3$H]dopamine and [$^3$H]dopa in various regions of the brain. *J Neurochem* 1966;13:655–669.
24. Seale TW, Abla KA, Shamim MT, Carney JM, Daly JW. 3,7-Dimethyl-1-propargylxanthine: a potent and selective in vivo antagonist of adenosine analogs. *Life Sci* 1988;43:1671–1684.
25. Chalmers DT, McCulloch J. Selective alterations in glutamate receptor subtypes after unilateral orbital enucleation. *Brain Res* 1991;540:255–265.
26. Lund RD. Synaptic patterns of the superficial layers of the superior colliculus of rat. *J Comp Neurol* 1969;135:179–208.
27. Toga AW, Collins RC. Metabolic response of optic centers to visual stimuli in the albino rat: anatomical and physiological considerations. *J Comp Neurol* 1981;199: 443–464.
28. Nagasawa H, Araki T, Kogure K. Alteration of adenosine $A_1$ receptor binding in the postischaemic rat brain. *Neuroreport* 1994;5:1453–1456.


# Iodine-123-5-Iodo-6-Nitroquipazine: SPECT Radiotracer to Image the Serotonin Transporter


William J. Jagust, Jamie L. Eberling, Anat Biegon, Scott E. Taylor, Henry F. VanBrocklin, Shaun Jordan, Stephen M. Hanrahan, Jeffrey A. Roberts, Kathleen M. Brennan and Chester A. Mathis

*Center for Functional Imaging, Lawrence Berkeley Laboratory, Berkeley, California; Department of Neurology and California Primate Research Center, University of California, Davis, California; Pharmos Corporation, Rehovot, Israel; and Department of Radiology, University of Pittsburgh, Pittsburgh, Pennsylvania*



Because serotonergic function has been implicated in the pathophysiology of a number of diseases of the nervous system, efforts to image this system in vivo have received considerable recent attention. Promising preliminary results with the tracer 5-iodo-6-nitroquipazine (INQUIP) have prompted us to perform further studies designed to validate the use of the tracer as an in vivo ligand for the serotonin transporter. **Methods:** We studied six adult macaca mulatta in eight experiments which involved SPECT imaging at 17 to 24 hr post-tracer injection, including three experiments with coinjection of the $^{123}$I- and $^{125}$I-radiolabeled tracer for direct comparison of autoradiography and SPECT, and three experiments in which animals were lesioned with the serotonergic neurotoxin (±)3,4-methylenedioxymethamphetamine (MDMA). In addition, we evaluated the metabolism of the tracer in the brain and periphery. **Results:** SPECT images obtained at 17 and 24 hr reflected the known pattern of distribution of serotonin transporters and also showed close correspondence to the autoradiograms. Ratios of binding in the brainstem to binding in the cerebellum were close to 3 at 17 hr. Autoradiograms from an MDMA-treated animal showed up to 95% reductions of binding, while the SPECT data showed smaller reductions. Virtually all of the tracer in the brain stem was in the form of unmetabolized parent compound, but plasma showed rapid peripheral metabolism of the tracer. **Conclusion:** These results demonstrate that INQUIP SPECT images are sensitive measures of in vivo binding to the serotonin transporter, and support the further development of the tracer as a method for the in vivo study of serotonergic neurons in humans.



**Key Words:** iodine-123-5-iodo-6-nitroquipazine; serotonin transporter

**J Nucl Med 1996; 37:1207–1214**


Analysis of serotonergic (5-hydroxytryptamine, 5-HT) components of the nervous system is potentially important in the understanding of a number of pathological conditions. Serotonergic neurons degenerate in both Alzheimer's disease and Parkinson's disease (*1,2*), and reductions in serotonergic function have been linked to the presence of depression in Parkinson's disease (*3*) and to specific behavioral characteristics in Alzheimer's disease (*4*). Differential degeneration of this neurotransmitter system may thus play a role in defining the clinical heterogeneity of these diseases and in producing distinguishing features which have been labeled as subtypes of the


Received May 10, 1995; revision accepted Aug. 16, 1995.



For correspondence or reprints contact: William J. Jagust, MD, Center for Functional Imaging, 55-121, Lawrence Berkeley Laboratory, Berkeley, CA 94720.